https://doi.org/10.15407/ujpe69.11.839

L. JENKOVSZKY

Bogolyubov Institute for Theoretical Physics, Nat. Acad. of Sci. of Ukraine
(14b, Metrolohichna Str., Kyiv 03680, Ukraine; e-mail: jenk@bitp.kiev.ua)

MINIMUM (DIP) AND MAXIMUM (BUMP) IN PROTON'S SINGLE DIFFRACTIVE DISSOCIATION AT THE LHC[1]

A dip-bump structure in the squared four-momentum transfer (t) distribution of proton's single and double diffractive distributions is predicted around $t \approx -4$ GeV^2 for single diffractive distribution at LHC energies.

K e y w o r d s: dip-bump structure, squared four-momentum transfer, LHC, proton's diffractive distributions.

1. Introduction. Single, Double, and Central Diffractive Dissociation

Measurements of single (SD), double (DD) and central (CD) diffraction dissociation distributitions is among the priorities of the LHC research program. As for now, a lot of studies of high-energy diffraction dissociation physics were performed at different research programs, e..g., at the Fermilab (Tevatron) or the LHC (ALICE, SPS, ...). Back in the 2000s, K. Goulianos, in a series of papers [1] introduced the theoretical approach to calculate the cross sections for single, double, and central diffractions.

The basic configurations of reactions with diffractive dissociation (DD) are listed below and shown in Fig. 1. Each one is characterized by large rapidity gaps corresponding to the exchange of a trajectory with vacuum quantum numbers (Pomeron). Multi-gap reactions with multi-pomeron exchanges are also possible, when the incoming energy is large enough.

Starting from the 70-ies, DD was intensively theoretically studied. At the Fermilab, a rich spectrum of resonances in missing masses was revived, still waiting for a better physical interpretation.

An approach based on the Regge-pole factorization was developed in a series of papers [2] see [5] and references therein, where single- and double DD were studied with emphases on resonances in missing masses treated on the basis of an original duality-based model.

In the present paper we continue our program focused on the resonance production in missing masses, this time in the framework of the of the Goulianos–Ciesielski model [3], modified by including resonances in missing masses. A novel development is the study of a possible dip-bump structure is SD and DD.

We consider diffraction dissociation with configurations shown in Fig. 1 and listed below:

$$\text{Elastic (1): } pp \to pp, \tag{1}$$

$$\text{SD (2): } pp \to pX(pY), \tag{2}$$

$$\text{DD (3): } pp \to XY, \tag{3}$$

$$\text{CD (DPE) (4): } pp \to pZp, \tag{4}$$

$$\text{CD}_\text{S} \text{ (5): } pp \to XZp, \tag{5}$$

$$\text{CD}_\text{D} \text{ (6): } pp \to XZY, \tag{6}$$

where X and Y represent diffraction dissociated protons (nucleon resonances), and Z are diffraction produced mesons in the central system. Note that SD (2)

Citation: Jenkovszky L. Minimum (dip) and maximum (bump) in proton's single diffractive dissociation at the LHC. *Ukr. J. Phys.* **69**, No. 11, 839 (2024). https://doi.org/10.15407/ujpe69.11.839.

[1] This work is based on the results presented at the 2024 "New Trends in High-Energy and Low-x Physics" Conference.

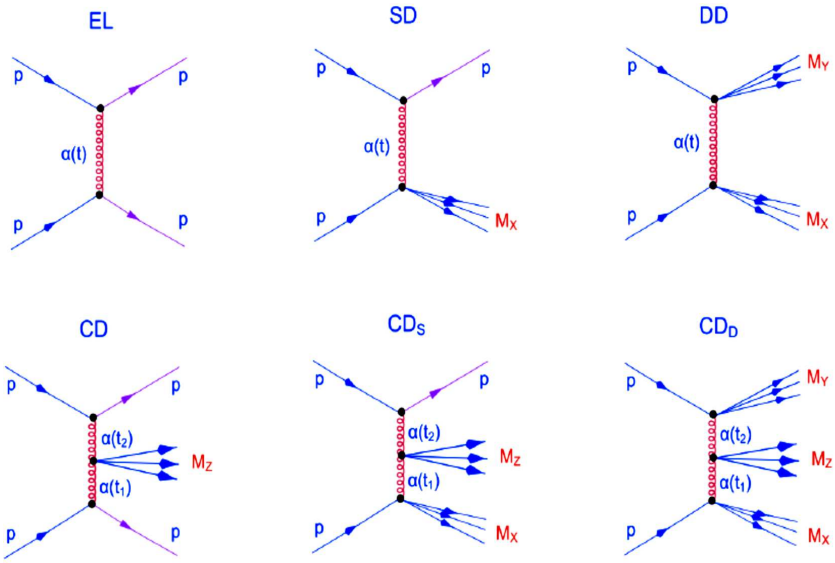

Fig. 1. Diagrams of elastic scattering (EL) and diffraction dissociation (single, double, and central)

implies two symmetric reactions, i.e., $p+p' \to X+p'$ and $p+p' \to p+X$. Schematically, those processes are shown in Fig. 1. Many more diffraction dissociation configurations (*e.g.,* those with multi-Pomeron exchanges) are possible.

2. The Model

The differential cross section for SD, DD, and CD can be written as [1, 3].

2.1. DD

Assuming the Regge factorization, the DD cross section may be obtained from the SD and elastic scattering cross section:

$$\frac{d^3\sigma_{\rm DD}}{dtd\xi_1 d\xi_2} = \frac{1}{d\sigma_{el}/dt}\frac{d^2\sigma_{\rm SD1}}{dtd\xi_1}\frac{d^2\sigma_{\rm SD2}}{dtd\xi_2} =$$
$$= \left\| \frac{d\sigma_{el}}{dt} = \frac{\beta^4(t)}{16\pi}\left(\frac{s}{s_0}\right)^{2\alpha(t)-2} \right\| =$$
$$= \frac{1}{N(s)}\left[\frac{s/s_0}{16\pi}\left(\frac{s\xi_1\xi_2}{s_0}\right)^{1-2\alpha(t)}\right] \times$$
$$\times \sigma_{1T}^{Pp}(s\xi_1)\sigma_{2T}^{Pp}(s\xi_2) \qquad (7)$$

and, for M^2 variable:

$$\frac{d^3\sigma_{\rm DD}}{dtdM_1^2 dM_2^2} = \frac{1}{d\sigma_{el}/dt}\frac{d^2\sigma_{\rm SD1}}{dtdM_1^2}\frac{d^2\sigma_{\rm SD2}}{dtdM_2^2} =$$
$$= \frac{1}{N(s)}\left[\frac{1}{16\pi M_1^2 M_2^2}\left(\frac{M_1^2 M_2^2}{s\, s_0}\right)^{2-2\alpha(t)}\right] \times$$
$$\times \sigma_{1T}^{Pp}(M_1^2)\sigma_{2T}^{Pp}(M_2^2), \qquad (8)$$

where σ_{iT}^{Pp} is the total Pomeron-proton cross section for each vertices, $i = 1, 2$.

2.2. CD

Using factorization, the CD cross section can be written as follows:

$$\frac{d^4\sigma_{\rm CD}}{dt_1 dt_2 d\xi_1 d\xi_2} = \frac{1}{\sigma_T^{p\bar{p}}}\frac{d^2\sigma_{\rm SD1}}{dt_1 d\xi_1}\frac{d^2\sigma_{\rm SD2}}{dt_2 d\xi_2} =$$
$$= \left\| \sigma_T^{p\bar{p}} = \beta^2(0)\left(\frac{s}{s_0}\right)^{\alpha(0)-1} \right\| =$$
$$= \frac{1}{N(s)\beta^2(0)(s/s_0)^{\alpha(0)-1}}\left[\frac{\beta^2(t_1)}{16\pi}{\xi_1}^{1-2\alpha(t_1)}\right] \times$$
$$\times \left[\frac{\beta^2(t_2)}{16\pi}{\xi_2}^{1-2\alpha(t_2)}\right]\kappa\,\sigma_T^{PP}(s\xi_1\xi_2), \qquad (9)$$

where σ_T^{PP} is the total Pomeron-Pomeron cross section.

3. Resonances in Missing Masses

The above model [3] is valid for large, Regge behaved missing masses. Our innovation is in the extension of the model valid also in the region of moderate M_i^2, dominated by resonances. The idea [2] is

based on duality, by which resonances the direct channel are produced by the pole decomposition of the dual amplitude, dominated by "reggeized" Breit–Wigner poles with non-linear, complex direct-channel Regge trajectories, providing for finite widths of resonances. The expressions in curly and square brackets of the above equations can be interpreted as the Pomeron-proton total cross section σ^{Pp} and so-called Pomeron fluxes f_{Pp}, emitted by the diffractively scattered proton. Regge-behaved total proton-Pomeron cross sections are used in most of the papers on the subject. This cross section will be replaced by a reggeized dual Breit–Wigner model introduced in [2], reproducing direct-channel resonances.

The $\gamma^* p$ total cross section is related to the structure function by

$$F_2(x,Q^2) = \frac{Q^2(1-x)}{4\pi\alpha(1+4m^2x^2/Q^2)} t\sigma_t^{\gamma^* p}, \tag{10}$$

where α is the fine structure constant, $Q^2 = -q^2$, and $x = \frac{Q^2}{2p\cdot q}$ is the Bjorken variable. Since $M^2 = (p+q)^2 = p^2+q^2+2p\cdot q$, $p\cdot q = \frac{1}{2}(M^2+Q^2-m_p^2)$, where m_p is the proton mass.

Alternatively,

$$\sigma_t^{\gamma^* p}(x,Q^2) = \frac{8\pi}{P_{\rm CM}\sqrt{s}} \operatorname{Im} A^{\gamma^* p}(s(x,Q^2), t=0, Q^2). \tag{11}$$

where $P_{\rm CM}$ is the absolute value of center of mass momentum of the reaction, $P_{\rm CM} = \frac{s-m^2}{2(1-x)} \times \times \sqrt{\frac{1+4m_p^2x^2/Q^2}{s}}$ for DIS with $s = (p+q)^2 \equiv M^2$. Thus, we have

$$F_2(x,Q^2) = \frac{4Q^2(1-x)^2}{\alpha\,(s-m^2)\,(1+4m^2x^2/Q^2)^{3/2}} \times \times \operatorname{Im} A^{\gamma^* p}(s(x,Q^2), t=0, Q^2). \tag{12}$$

A Reggeon (here, the Pomeron) is similar to the photon. Hence, Pomeron-proton interaction is similar to photon-proton DIS, where $-Q^2 = q^2 \to t$ and $s = W^2 \to M^2$. Thus, replacing the virtual photon to a Pomeron. Substituting $Q^2 = -t$, $s = M^2$, we obtain:

$$F_2(M^2,t) = \frac{-t4(1-x)^2}{\alpha\left(M^2-m_p^2\right)\left(1+4m_p^2x^2/-t\right)^{3/2}} \times \times \operatorname{Im} A^{Pp}(M^2,t), \tag{13}$$

where $x \equiv x(M^2,t)$ and, instead of x, we use M^2 as a variable.

$F_2 = \nu W_2$, where $\nu = \frac{-t}{2m_p x}$. The contribution of the Pp vertex to the differential cross section of the diffractive processes is $\tilde{W}^{Pp} = \frac{W_2}{2m_p}$.

3.1. Pomeron-Pomeron scattering

Most of the studies on diffraction dissociation, single, double, and central, use the triple Reggeon formalism. This approach is useful in the smooth Regge region, beyond the resonance region, but is not applicable for the production of low masses which is dominated by resonances. We solve this problem by using a dual model.

The one-by-one account for the single resonances is possible, but not economic for the calculation of cross section, to which a sequence of many resonances contributes at low masses. These resonances overlap and gradually disappear in the continuum at higher masses.

For our purpose of central production, the direct-channel pole decomposition of the dual amplitude $A(M^2,t)$ is relevant. Different trajectories $\alpha_i(M^2)$ contribute to this amplitude, with $\alpha_i(M^2)$ a non-linear, complex Regge trajectory in the Pomeron-Pomeron system,

$$A(M^2,t) = a \sum_{i=f,P} \sum_J \frac{[f_i(t)]^{J+2}}{J-\alpha_i(M^2)}. \tag{14}$$

The pole decomposition of the dual amplitude $A(M^2,t)$ is shown in Eq. (14), with t the squared momentum transfer in the $PP \to PP$ reaction. The index i sums over the trajectories which contribute to the amplitude. Within each trajectory, the second sum extends over the bound states of spin J. The prefactor a in Eq. (14) is of numerical value $a = 1\ \text{GeV}^{-2} = 0.389$ mb.

The pole residue $f(t)$ appearing in the $PP \to PP$ system is fixed by the dual model, in particular, by the compatibility of its Regge asymptotics with Bjorken scaling and reads

$$f(t) = (1-t/t_0)^{-2}, \tag{15}$$

where t_0 is a parameter to be fitted to the data. However, due to the absence of data so far, we set $t_0 = 0.71\ \text{GeV}^2$ for the moment as in the proton elastic form factor.

The imaginary part of the amplitude $A(M^2,t)$ given in Eq. (14) is defined by

$$\operatorname{Im} A(M^2,t) = \\ = a\sum_{i=f,P}\sum_{J}\frac{[f_i(t)]^{J+2}\operatorname{Im}\alpha_i(M^2)}{(J-\operatorname{Re}\alpha_i(M^2))^2+(\operatorname{Im}\alpha_i(M^2))^2}. \quad (16)$$

Recall that the amplitude A and the cross section σ_t carry dimensions of mb due to the dimensional parameter a discussed above. The Pomeron-Pomeron channel, $PP \to M^2$, couples to the Pomeron and f channels dictated by the conservation of quantum numbers. In order to calculate the PP cross section, we, therefore, consider the trajectories associated to the $f_0(980)$ and to the $f_2(1270)$ resonance, and the Pomeron trajectory.

3.2. Inclusion of resonances in the model

As we mentioned above, the Goulianos model is valid only for large M^2 and not for the resonance region (roughly, $M \sim$ 1–4 GeV). Therefore, the expression in curly brackets should be replaced by reggeized dual Breit–Wigner resonances.

Using the transition factors, we get the following extension of single and double diffractive dissociations:

$$\frac{d^2\sigma_{\rm SD}}{dtdM^2} = \frac{1}{N(s)}f_{P/p}(M^2,t,s)\cdot\sigma_T^{Pp}(M^2,t,s), \quad (17)$$

$$\frac{d^3\sigma_{\rm DD}}{dtdM_1^2dM_2^2} = \frac{1}{N(s)}f_{P/p}(M_1^2M_2^2,t,s)\times \\ \times\sigma_T^{Pp}(M_1^2,t,s)\,\sigma_T^{Pp}(M_2^2,t,s), \quad (18)$$

where the Pomeron-proton total cross section σ_T^{Pp} is the sum of N^* resonances ($\sigma_{\rm Res}^{Pp}$) and the background corresponding to a smooth function:

$$\sigma_T^{Pp}(M^2,t) = A_{\rm res}\cdot\sigma_{\rm Res}^{Pp}(M^2,t)+\sigma_{Bg}^{Pp}(M^2), \quad (19)$$

the background is:

$$\sigma_{Bg}^{Pp}(M^2) = a\cdot\kappa\cdot\beta^2(0)\cdot(M^2)^{\epsilon}, \quad (20)$$

and $A_{\rm res}$ is the free parameter obtained by the fits. In Eq. (19), we write $\sigma_{\rm Res}^{Pp}$ assuming that Eq. (11), we replace the virtual photon with the Pomeron and apply the substitutions $-Q^2 = t$, $s = M^2$. With these manipulations, we can write:

$$\sigma_{\rm Res}^{Pp}(M^2,t) = \frac{8\pi}{P_{\rm CM}\sqrt{M^2}}\operatorname{Im} A(M^2,t), \quad (21)$$

$$P_{\rm CM} = \frac{M^2-m_p^2}{2(1-x)}\sqrt{\frac{1-4m_p^2x^2/t}{M^2}}, \quad (22)$$

$$\operatorname{Im} A(M^2,t) = \\ = a\sum_{n=1,6}\frac{[f(t)]^{2(n+1)}\operatorname{Im}\alpha_{N^*}(M^2)}{(2n+0.5-\operatorname{Re}\alpha_{N^*}(M^2))^2+(\operatorname{Im}\alpha_{N^*}(M^2))^2}, \quad (23)$$

where $m_p = 0.938$ GeV is the proton mass, $a = 0.3894$ mb gives us the cross section in [mb], $x(M^2,t) = \frac{-t}{M^2-m_p^2-t}$, and $\alpha_{N^*}(M^2)$ is a direct-channel complex, non-linear Regge trajectory .

Using the central diffraction dissociation transition equation Eq. (9), one can write:

$$\frac{d^4\sigma_{CD}}{dt_1dt_2d\xi_1d\xi_2} = \frac{1}{N(s)\beta^2(0)(s/s_0)^{\alpha(0)-1}}\times \\ \times f_{P/p}(\xi_1,t_1)f_{P/p}(\xi_2,t_2)\cdot\kappa\cdot\sigma_T^{PP}(s\xi_1\xi_2,t_1,t_2). \quad (24)$$

4. Compilation of the Basic Formulae

This section contains a compilation of the main equations used in the calculations and the fitting procedure.

The single diffraction dissociation (SD) differential cross section is:

$$\frac{d^2\sigma_{\rm SD}}{dtd\xi} = \frac{1}{N(s)}\left[\frac{\beta^2(t)}{16\pi}(\xi)^{1-2\alpha(t)}\right]\sigma_T^{Pp}(s\xi,t), \quad (25)$$

$$\frac{d^2\sigma_{\rm SD}}{dtdM^2} = \frac{1}{N(s)}\left[\frac{1}{M^2}\frac{\beta^2(t)}{16\pi}\left(\frac{M^2}{s}\right)^{2-2\alpha(t)}\right]\sigma_T^{Pp}(M^2,t), \quad (26)$$

and for the $\log_{10}\xi$ variable is:

$$\frac{d^2\sigma_{\rm SD}}{dtd\log_{10}\xi} = \ln 10\cdot\xi\cdot\frac{d^2\sigma_{\rm SD}}{dtd\xi}(\xi,t,s), \quad (27)$$

where $\xi\in[\log_{10}(1.4/s);\ \log_{10}0.05]$.

The double diffraction dissociation (DD) differential cross section:

$$\frac{d^3\sigma_{\rm DD}}{dtdM_1^2dM_2^2} = \frac{1}{N(s)}\left[\frac{1}{16\pi M_1^2M_2^2}\left(\frac{M_1^2M_2^2}{ss_0}\right)^{2-2\alpha(t)}\right]\times \\ \times\sigma_T^{Pp}(M_1^2,t)\sigma_T^{Pp}(M_2^2,t). \quad (28)$$

The central diffraction dissociation (CD) differential cross section is:

$$\frac{d^4\sigma_{\rm CD}}{dt_1dt_2d\xi_1d\xi_2} = \frac{1}{N(s)\beta^2(0)(s/s_0)^{\alpha(0)-1}}\times$$

$$\times \left[\frac{\beta^2(t_1)}{16\pi}{\xi_1}^{1-2\alpha(t_1)}\right]\left[\frac{\beta^2(t_2)}{16\pi}{\xi_2}^{1-2\alpha(t_2)}\right]\times$$
$$\times\,\kappa\cdot\sigma_T^{PP}(s\xi_1\xi_2,t). \tag{29}$$

The slope B of the cone is defined as follows:

$$B=\frac{d}{dt}\frac{d\sigma}{dt}. \tag{30}$$

The cross-integrated cross sections vs. M^2 (vs. t) are calculated as:

$$\frac{d\sigma_{\rm SD}}{dM^2}=\int\limits_{-1}^{0}\frac{d^2\sigma_{\rm SD}}{dtdM^2}\,dt, \tag{31}$$

$$\frac{d\sigma_{\rm SD}}{dt}=\int\limits_{1.4}^{0.05s}\frac{d^2\sigma_{\rm SD}}{dtdM^2}\,dM^2, \tag{32}$$

for the case of SD, and

$$\frac{d^2\sigma_{\rm DD}}{dM_1^2dM_2^2}=\int\limits_{-1}^{0}\frac{d^3\sigma_{\rm DD}}{dtdM_1^2dM_2^2}\,dt, \tag{33}$$

$$\frac{d\sigma_{\rm DD}}{dt}=\int\limits_{1.4}^{0.05s/1.4}dM_1^2\int\limits_{1.4}^{0.05s/M_1^2}\frac{d^3\sigma_{\rm DD}}{dtdM_1^2dM_2^2}\,dM_2^2. \tag{34}$$

for the case of DD.

We also calculated the cross integrated cross section vs. $\log_{10}\xi$ for SD:

$$\frac{d\sigma_{\rm SD}}{d\log_{10}\xi}=\int\limits_{-1}^{0}\frac{d^2\sigma_{\rm SD}}{dtd\log_{10}\xi}\,dt. \tag{35}$$

The fully integrated cross sections are given by the further equations:

$$\sigma_{\rm SD}=\int\limits_{1.4}^{0.05s}dM^2\int\limits_{-1}^{0}dt\frac{d^2\sigma_{\rm SD}}{dM^2dt}, \tag{36}$$

$$\sigma_{\rm DD}=\int\limits_{1.4}^{0.05s}dM_1^2\int\limits_{1.4}^{0.05s/M_1^2}dM_2^2\int\limits_{-1}^{0}\frac{d^3\sigma_{\rm DD}}{dtdM_1^2dM_2^2}\,dt, \tag{37}$$

$$\sigma_{\rm CD}=\int\limits_{1.4/s}^{0.05}d\xi_1\int\limits_{1.4/s}^{0.05/\xi_1}d\xi_2\int\limits_{-1}^{0}dt_1\int\limits_{-1}^{0}dt_2\frac{d\sigma_{\rm CD}^4}{dt_1dt_2d\xi_1d\xi_2}. \tag{38}$$

5. Dip and Bump

High-energy hadron scattering is characterized by a forward peak followed by possible dips and bumps. The slope of the forward peak shrinks with energy and is related to the radii of the scattering particles. Multiple dips and bumps appear in nuclei scattering, but only a single structure is seen in pp scattering.

Proton elastic scattering and diffractive dissociation, single (SD) and double (DD) are closely related reactions. They were studied at the ISR, SPS, FNAL and are being studied at the LHC. Till now, no structures were seen in the differential cross sections of SD or DD.

For SD and DD, we use the model developed in a number of papers for elastic scattering, see [5] and earlier references. The scattering amplitude in that model is similar to that of elastic scattering, the elastic vertices being replaced by DIS structure functions.

The position of the structures in t depends on the energy, missing masses as well and are sensitive to the slopes of the SD and DD cones. The general trend is that the decreasing slope moves the structures towards larger $-t$. Most of the present measurements at the LHC are in the region of large missing masses and small t. With the present paper, we encourage experimentalists to measure the $-t$ dependence of SD and DD beyond several GeV^2 for varying missing masses.

6. Dip and Bump in Elastic Scattering

The dipole pomeron scattering amplitude is defined as [4]

$$A_P(s,t)=\frac{d}{d\alpha_P}\Big[{\rm e}^{-i\pi\alpha_P/2}G(\alpha_P)\Big(s/s_{0P}\Big)^{\alpha_P}\Big]=$$
$$={\rm e}^{-i\pi\alpha_P(t)/2}(s/s_{0P})^{\alpha_P(t)}\times$$
$$\times\Big[G'(\alpha_P)+\Big(L_P-i\pi/2\Big)G(\alpha_P)\Big], \tag{39}$$

where $L_P=\ln(s/s_{0P})$. Since the first term in squared brackets determines the shape of the cone, one fixes

$$G'(\alpha_P)=a_P{\rm e}^{b_P[\alpha_P-\alpha_{0P}]}, \tag{40}$$

where α_{0P} is the intercept of α_P. $G(\alpha_P)$ is recovered by integration:

$$G(\alpha_P)=\int d\alpha_PG'(\alpha_P)=$$
$$=a_P\Big({\rm e}^{b_P[\alpha_P-\alpha_{0P}]}/b_P-\gamma_P\Big). \tag{41}$$

The integration constant γ alone has no physical meaning, but its numerical value affects strongly the fits.

From the LHC energies on, the contribution from secondary Reggeons can be neglected, and one can rely on the Pomeron contribution only, eventually supplied by the odderon,

$$A^{pp}_{p\bar{p}}(s,t) \;=\; A_P(s,t) \mp A_O(s,t), \tag{42}$$

$$A_O(s,t) = -iA_{P\to O}(s,t). \tag{43}$$

By introducing the parameter $\epsilon_P = \gamma_P b_P$, the pomeron amplitude Eq. (39) can be rewritten in a geometrical form:

$$A_P(s,t) = i\frac{a_P}{b_P}\left(\frac{s}{s_{0P}}\right)^{\alpha_{0P}} e^{-\frac{i\pi}{2}(\alpha_{0P}-1)} \times$$
$$\times \left[r^2_{1P}\mathrm{e}^{r^2_{1P}[\alpha_P(t)-\alpha_{0P}]} - \varepsilon_P r^2_{2P}\mathrm{e}^{r^2_{2P}[\alpha_P(t)-\alpha_{0P}]}\right], \tag{44}$$

where $r^2_{1P}(s) = b_P + L_P - i\pi/2$ and $r^2_{2P}(s) = L_P - - i\pi/2$.

We use the norm where:

$$\sigma_{\mathrm{tot}}(s) = \frac{4\pi}{s}\,\mathrm{Im}\,A(s,t=0), \tag{45}$$

$$\frac{\mathrm{d}\sigma_{el}}{\mathrm{d}t}(s,t) = \frac{\pi}{s^2}\left|A\left(s,t\right)\right|^2 . \tag{46}$$

Fits to the data by the Regge dipole pomeron and odderon can be found, e.g., in papers [5, 6].

A dipole amplitude generates a dip-bump structure in the differential cross section. The position of the minimum (dip) and the maximum (bump) of the elastic differential cross section are

$$-t_{\mathrm{dip}} = \frac{1}{\alpha' b}\ln\frac{(b+L)}{\gamma bL} \tag{47}$$

and

$$-t_{\mathrm{bump}} = \frac{1}{\alpha' b}\ln\frac{\left[4(b+L)^2+\pi^2\right]}{\gamma b(4L^2+\pi^2)}. \tag{48}$$

The positions of the dip and bump depend on poorly known slope b of the connected with the differential cross section. The smaller the value of b, the higher the $|t|$ value, where the dip-bump structure appears. Thus, in the picture provided by the dipole Regge framework, it is natural to expect that, in single diffractive dissociation, a possible dip-bump structure appears at higher $|t|$ values, than it does in elastic scattering.

It is known that, in pp elastic scattering, the slope of the diffraction cone is energy-dependent and rises with increasing energy. At the same time, as the energy rises, the position of the dip-bump structure moves to smaller $-t$ values. The energy-dependent slope is given by the derivative of the logarithm of the differential cross section at $t = 0$. In the case of a single diffraction dissociation, the slope of the differential cross section depends not only on the energy, but also on the mass squared of the produced hadronic system as discussed above. Thus, in parallel to the elastic scattering it is not surprising that the dip-bump structure of the differential cross section of single diffraction, through the mass dependence moves in $-t$.

7. From Elastic Scattering to Single Diffractive Dissociation (SD)

To generate a dip-bump structure in single diffraction dissociation, we introduce a dipole pomeron and odderon exchange to the differential cross section.

In the triple Regge approach, the triple PPP exchange contribution to the SD differential cross section is

$$\frac{d^2\sigma_{\mathrm{SD}}}{dtdM^2} = \frac{1}{16\pi^2}\frac{1}{M^2}g^2_{Ppp}(t)\left(s/M^2\right)^{2\alpha_P(t)-2} \times$$
$$\times\, g_{PPP}(t)g_{Ppp}(0).(M^2)^{\delta_P}. \tag{49}$$

It is nearly t independent, thus $g_{PPP}(t) \simeq g_{PPP}(0)$. We have, for the t-dependent part of the SD amplitude:

$$A^{\mathrm{SP}}_{\mathrm{SD}}(s,M^2,\alpha_P) \sim \eta(\alpha_P)G_P(\alpha_P)(s/M^2)^{\alpha_P}, \tag{50}$$

where the t-dependence resulting from $g_{Ppp}(t)$ is accounted for by $G(\alpha)$. Hence, the t-dependent part of the dipole pomeron amplitude is:

$$A^{\mathrm{DP}}_{\mathrm{SD}}(s,M^2,\alpha_P) = \frac{d}{d\alpha_P}A^{\mathrm{SP}}_{\mathrm{SD}}(s,M^2,\alpha) \sim \mathrm{e}^{-i\pi\alpha/2} \times$$
$$\times\,(s/M^2)^{\alpha}\left[G'_P(\alpha_P) + \Big(L_{\mathrm{SD}} - i\pi/2\Big)G_P(\alpha_P)\right], \tag{51}$$

where

$$L_{\mathrm{SD}} \equiv \ln\left(s/M^2\right). \tag{52}$$

The resulting double differential cross section for the SD process is

$$\frac{d^2\sigma^{PPP}_{\mathrm{SD}}}{dtdM^2} = \frac{1}{M^2}\Bigg(G'^2_P(\alpha_P) + 2L_{\mathrm{SD}}G_P(\alpha_P)G'_P(\alpha_P) +$$

$$+ G_P^2(\alpha_P)\left(L_{\rm SD}^2 + \frac{\pi^2}{4}\right)\Big)(s/M^2)^{2\alpha_P(t)-2}\sigma^{Pp}(M^2), \quad (53)$$

where

$$\sigma^{Pp}(M^2) = g_{PPP}g_{Ppp}(0)(M^2 t)^{\alpha(0)-1}. \quad (54)$$

By using the proton relative momentum loss variable $\xi = M^2/s$, we get:

$$\frac{d^2\sigma_{\rm SD}^{PPP}}{dtd\xi} = \Big(G'^2(\alpha) + 2L_{\rm SD}G(\alpha)G'(\alpha) + G^2(\alpha) \times$$
$$\times \left(L_{\rm SD}^2 + \frac{\pi^2}{4}\right)\Big)\xi^{1-2\alpha(t)}\sigma^{Pp}(s\xi), \quad (55)$$

where

$$L_{\rm SD} \equiv -\ln\xi. \quad (56)$$

Using Eq. (40), Eq. (41), and Eq. (53), one finds the positions of the dip and the bump in the t dependence of the SD differential cross section:

$$t_{\rm dip}^{\rm SD} = \frac{1}{\alpha' b}\ln\frac{\gamma b L_{\rm SD}}{b + L}, \quad (57)$$

$$t_{\rm bump}^{\rm SD} = \frac{1}{\alpha' b}\ln\frac{\gamma b(4L_{\rm SD}^2 + \pi^2)}{4(b + L_{\rm SD})^2 + \pi^2}. \quad (58)$$

We include also the contribution of the odderon in the odderon-odderon-pomeron (OOP) triple exchange. In standard triple Regge formalism it takes the form:

$$\frac{d^2\sigma_{\rm SD}}{dtdM^2} = \frac{1}{16\pi^2}\frac{1}{M^2}g_{Opp}^2(t)(s/M^2)^{2\alpha_O(t)-2} \times$$
$$\times\, g_{OOP}(t)g_{Ppp}(0)(M^2)^{\delta_O}. \quad (59)$$

We use its dipole form (the derivation is the same as in case of the dipole PPP contribution):

$$\frac{d^2\sigma_{\rm SD}^{OOO}}{dtdM^2} = \frac{1}{M^2}\Big(G_O'^2(\alpha_O) + 2L_{\rm SD}G_O(\alpha_O)G_O'(\alpha_O) +$$
$$+ G_O^2(\alpha_O)\left(L_{\rm SD}^2 + \frac{\pi^2}{4}\right)\Big)(s/M^2)^{2\alpha_O(t)-2}\sigma^{Pp}(M^2), \quad (60)$$

where σ^{Pp} is given by Eq. (54), and the possible difference between g_{OOP} and g_{PPP} is accounted by a_O. The dip and bump positions in the dipole OOP contribution are given by Eq. (57) and Eq. (58).

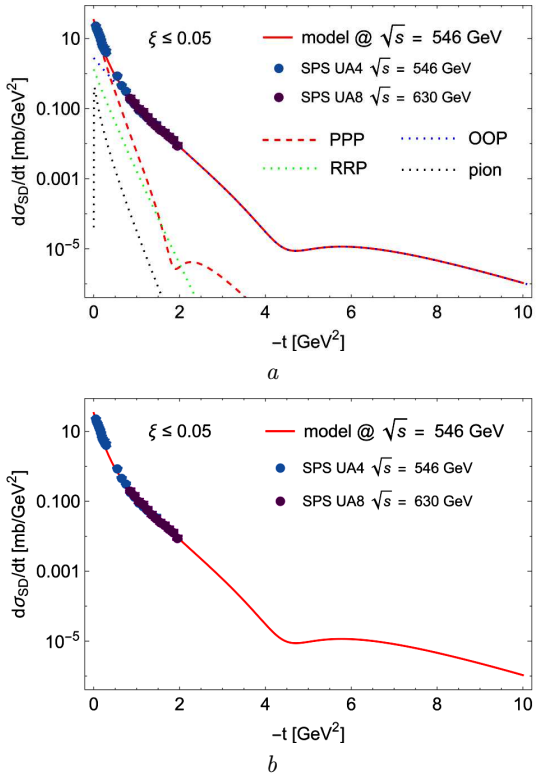

Fig. 2. Predicted dip-bump structure in the t distribution of the ξ integrated differential cross section of single diffraction dissociation at $\sqrt{s} = 546$ GeV (a) with the different contributions shown and (b) without

The complete model for double differential cross section of SD is a sum of three triple Regge contribution appended by a pion exchange contribution:

$$\frac{d^2\sigma_{\rm SD}}{dtdM^2} = \frac{d^2\sigma_{\rm SD}^{PPP}}{dtdM^2} + \frac{d^2\sigma_{\rm SD}^{OOP}}{dtdM^2} + \frac{d^2\sigma_{\rm SD}^{RRP}}{dtdM^2} + \frac{d^2\sigma_{\rm SD}^{\pi}}{dtdM^2}. \quad (61)$$

The parameters a and b were fitted to the data. The parameter γ was fixed at values obtained in the analysis of the elastic scattering data. The intercepts of the pomeron and the odderon trajectories are 1, *i.e.* $\delta_P = \delta_O = 0$. The slopes of the pomeron and the odderon trajecories are fixed at the values obtained in the analysis of the elastic scattering data.

Interestingly, the DP Pomeron model of proton-proton SD produces properly rising total integrated cross sections with unit Pomeron intercept, i.e., with $\delta = 0$.

The predicted structures in the differential cross section at $\sqrt{s} = 546$ GeV, also integrated in ξ are below. Different contributions to the differential cross section are also shown. One can see that both the dipole PPP triple exchange and the dipole OOP triple exchange generate a dip-bump structure. The experimentally observable effect is expected from the OOP contribution.

8. Summary

We predict a dip followed by a dump in proton single diffractive dissociation around $t \approx -4$ GeV^{-2}. The prediction is sensitive to the poorly known slope of SD. Further studies, both theoretical and experimental are needed.

Useful collaboration with M.M. Mieskolainen, V. Rezoglazov, O. Skorenok, I. Szanyi at an early stage of this work is acknowledged.

My work was supported by EURIZON, Grant Agreement #EU-3031-A.

1. K. Goulianos. Diffractive interactions of hadrons at high energies. *Phys. Rep.* **101**, 170 (1983).
2. L.L. Jenkovszky, O.E. Kuprash, J.W. Lämsa, V.K. Magas, R. Orava. Dual-Regge approach to high-energy, low-mass diffraction dissociation. *Phys. Rev. D* **83**, 056014 (2011).
3. R. Ciesielski, K. Goulianos. MBR Monte Carlo simulation in PYTHIAS. arXiv:1205.1446.
4. L.L. Jenkovszky, A.N. Vall. Dipole Pomeron and *pp* scattering. *Czech. J. Phys. B* No. 4, 447 (1976).
5. László Jenkovszky, Rainer Schicker, I. Szanyi. Dip-bump structure in proton's single and diffractive dissociationm at the large hadron collider. *Universe* **10**, 208 (2022).
6. Wojciech Broniowski, László Jenkovszky, Enrique Ariola, István Szanyi. Hollowness in *pp* and $\bar{p}p$ scattering in a Regge model. *Phys. Rev. D* **98**, 074012-1 (2018).

Received 07.10.24

Л. Єнковський

МІНІМУМ (ПРОВАЛ) І МАКСИМУМ (ГОРБ) У ОДИНАРНІЙ ДИФРАКЦІЙНІЙ ДИСОЦІАЦІЇ ПРОТОНА НА LHC

Для одинарного дифракційного розподілу при енергіях прискорювача LHC передбачається існування структури провал-горб у квадраті функції розподілу в залежності від переданого 4-імпульса t при значенні $t \approx -4$ ГеВ^2 у процесах одинарної та подвійної дифракційної дисоціації протона.

Ключові слова: структура провал-горб, квадрат переданого чотириімпульса, LHC, дифракційна дисоціація протона.